Biochimica et Biophysica Acta 1818 (2012) 2917–2925

Contents lists available at SciVerse ScienceDirect

Biochimica et Biophysica Acta

journal homepage: www.elsevier.com/locate/bbamem

Anticancer mechanisms of action of two small amphipathic $\beta^{2,2}$-amino acid derivatives derived from antimicrobial peptides

Dominik Ausbacher [a], Gunbjørg Svineng [b], Terkel Hansen [a,1], Morten B. Strøm [a,*]

[a] Department of Pharmacy, Faculty of Health Sciences, University of Tromsø, 9037 Tromsø, Norway
[b] Department of Medical Biology, Faculty of Health Sciences, University of Tromsø, 9037 Tromsø, Norway

ARTICLE INFO

Article history:
Received 19 April 2012
Received in revised form 3 July 2012
Accepted 11 July 2012
Available online 20 July 2012

Keywords:
Antimicrobial peptide
Anticancer peptide
Apoptosis
Beta-amino acid
Caspases
Mitochondria

ABSTRACT

We have recently discovered that small antimicrobial $\beta^{2,2}$-amino acid derivatives (Mw<500) also display activity against cancer cells. To explore their drug potential, we have presently investigated the mechanisms of action of two derivatives BAA-1 (IC_{50} 8.1 μg/ml) and BAA-2 (IC_{50} 3.8 μg/ml) on Ramos human Burkitt's lymphoma cells. Studies using annexin-V-FITC/propidium iodide staining and flow cytometry revealed essential mechanistic differences, which was confirmed by screening for active caspases, investigation of mitochondrial membrane potential, and electron microscopy studies. Our results indicated that BAA-1 killed Ramos cells by destabilizing the cell membrane, whereas BAA-2 caused apoptosis by the mitochondrial-mediated pathway.

1. Introduction

Cancer is predicted to displace heart diseases as the leading cause of death worldwide, and is further globally estimated to double by the year 2020 and nearly triple by 2030 [1,2]. Natural products, a valuable source of drug lead compounds, are therefore extensively explored in the search for new anticancer agents, and a branch of the field of cationic antimicrobial peptides (AMPs) has already shown promising therapeutic potential in clinical trials [3–5]. Certain AMPs and AMP derived peptides are also known to possess anticancer properties. These anticancer peptides (ACPs) are unique compared to other cytostatic drugs by selectively interfering with cancer cells via a charge-triggered membrane disruptive mode of action [6]. There is additional evidence that ACPs can cause mitochondrial-mediated activation of apoptosis, stimulation of the host's immune system, and prevention of tumor angiogenesis [6]. Thus, by exploring these mechanisms of action, ACP based molecules with optimized potencies and pharmacokinetic properties may form a novel and promising approach in cancer therapy [7].

We have recently reported the antimicrobial activity of a series of small $\beta^{2,2}$-amino acid derivatives that were designed to confirm the pharmacophore model of short cationic AMPs, and that are especially potent against methicillin resistant *Staphylococcus aureus* (MRSA) and with low hemolytic activity [8,9]. The $\beta^{2,2}$-amino acid derivatives show important pharmacokinetic advantages compared to natural occurring AMPs by being much more stable against proteolytic degradation, and by being able to permeate phospholipid-vesicle barriers by passive diffusion and thereby resemble drug absorption across the intestinal epithelia [8,9]. During our studies we have recently discovered that some of these $\beta^{2,2}$-amino acid derivatives also display anticancer activity. High potency of one of the most promising derivatives BAA-2 (see Fig. 1) has been confirmed by screening it against 59 cancer cell lines at the National Cancer Institute (NCI) revealing IC_{50} values<4 μM (Strøm et al., unpublished results).

We have therefore in the current study continued our investigations and selected two $\beta^{2,2}$-amino acid derivatives, BAA-1 and BAA-2, for elucidation of parts of their anticancer mechanism of action (Fig. 1). BAA-1 was selected based on its elongated and flexible side-chain structure that was hypothesized to interact strongly with the phospholipid acyl-chain region of the cancer cell membrane, whereas BAA-2 was selected due to its much more rigid and bulky 2-naphthyl methylene side-chains that were hypothesized to cause a significant lateral distortion of the cancer cell membrane. However, the results revealed much larger differences in the mechanism of action of BAA-1 and BAA-2 than anticipated, and involved cell membrane disruption and mitochondria

Abbreviations: AIF, Apoptosis-inducing factor; AMP, antimicrobial peptide; ACP, anticancer peptide; DMSO, dimethyl sulfoxide; FBS, fetal bovine serum; FITC, fluorescein isothiocyanate; HBSS, Hank's balanced salt solution; Lfcin B, bovine lactoferricin; NCI, National Cancer Institute; PBS, phosphate buffered saline; PI, propidium iodide; SEM, scanning electron microscopy; TBTC, tributyltin chloride; TEM, transmission electron microscopy; TMRE, tetramethylrhodamine ethyl ester perchlorate

* Corresponding author. Tel.: +47 77 64 40 85; fax: +47 77 64 61 51.
E-mail address: morten.strom@uit.no (M.B. Strøm).
[1] Present address: Leibniz-Institut für Analytische Wissenschaften-ISAS-e.V. Otto-Hahn-Str. 6b, 44227 Dortmund, Germany.

0005-2736/$ – see front matter © 2012 Elsevier B.V. All rights reserved.
doi:10.1016/j.bbamem.2012.07.005

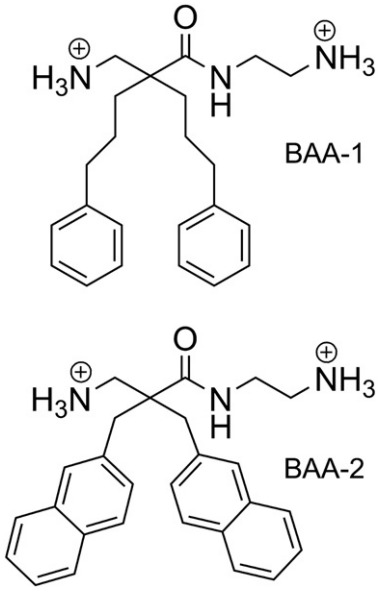

Fig. 1. Structures of the AMP derived $\beta^{2,2}$-amino acid derivatives BAA-1 and BAA-2.

mediated activation of caspases, which to our knowledge only has been reported for much larger ACPs [10–13]. The study presents the anticancer activity of BAA-1 and BAA-2 against human Burkitt's lymphoma cells (Ramos cells) utilizing a resazurin based cell viability assay for cell killing kinetics, and determination of cell death using flow cytometry and an annexin-V-FITC and propidium iodide (PI) protocol. In addition, screening for cellular caspase activity and assessment of the mitochondrial membrane potential were investigated together with scanning electron microscopy (SEM) and transmission electron microscopy (TEM) for providing insights into morphological changes of Ramos cells incubated with BAA-1 and BAA-2. Since *drug-likeness* as defined by the *Lipinski´s rule of five* [14] as well as concerns of cost efficiency were addressed when designing these $\beta^{2,2}$-amino acid derivatives, the present results add to their potential of forming a novel approach in the field of developing ACP-chemotherapeutic drugs.

2. Material and methods

2.1. BAA-1 and BAA-2 compounds

The $\beta^{2,2}$-amino acid derivatives BAA-1 and BAA-2 (Fig. 1) were synthesized as recently reported by our group [9]. The crude products were purified by preparative RP-HPLC and analysis with an analytical RP-HPLC C_{18}-column and UV detection at 214 nm and 254 nm showed purity > 95%.

2.2. Cell line

Ramos cells were cultivated in RPMI-1640 growth medium supplemented with 10% fetal bovine serum (FBS) (Sigma-Aldrich, St. Louis, MO, USA) and incubated in a 37 °C and 5% CO_2 humidified incubator. The cell line is tested regularly for mycoplasma infection and was identified as Ramos (RA.1) by STR analysis in February 2011.

2.3. Resazurin based viability and kinetic assay

A colorimetric cell viability assay with the resazurin based TOX-8 assay kit (Sigma-Aldrich, St. Louis, MO, USA) was used to evaluate cytotoxic effects. Volumes of 100 µl of the test compounds BAA-1 and BAA-2 in serum free RPMI-1640 medium were added to 96-well plates to obtain final concentrations ranging from 50 µg/ml to 0.25 µg/ml. RPMI-1640 medium was used as a negative control. After supplementing with 20 µl of the resazurin solution, Ramos cells were added immediately to reach a cell density of 2×10^5 cells/ml. The 96-well plates were incubated at 37 °C and the absorbance measured hourly with a multi-well spectrophotometer (VersaMax, Molecular devices, Sunnyvale, CA) at 570 nm and a reference wavelength at 600 nm. The cell survival rate was calculated as the ratio of the corrected background absorbance values of treated cells and the non-treated control cells. The half inhibitory concentrations (IC_{50}) were determined over a period of 8 h and finished with a final measurement at 24 h. Additional experiments with doxorubicin were performed to compare the obtained results with this established chemotherapeutic agent. Doxorubicin hydrochloride was used in final concentrations from 5.80 µg/ml to 6 ng/ml corresponding to approximately 5× the initial doxorubicin plasma concentration after bolus administration and plasma concentrations 1 h past injection [15]. Due to a slower mechanism of action of doxorubicin compared to BAA-1 and BAA-2, the assay was extended to 28 h. In order to avoid reduced viability of the Ramos cells due to culture conditions, the medium was supplemented with 0.5% FBS. The cells were incubated with doxorubicin for 24 h, subsequently resazurin was added and the cells were further incubated for an additional 4 h before the final read out.

The kinetic properties of BAA-1 and BAA-2 were evaluated using three different concentrations corresponding to 0.1×, 1× and 10× the determined IC_{50} values. Ramos cells were seeded in a 96-well plate, containing resazurin and the $\beta^{2,2}$-amino acid derivatives in different concentrations, and incubated under the same conditions as described above. The increase in absorbance of the reduced dye was recorded by a multi-well spectrophotometer at 570 nm and corrected for the reference wavelength at 600 nm.

2.4. Annexin V-FITC and propidium iodide assay

The assay was performed according to the manufacturer's protocol (APOAF, Sigma-Aldrich, St. Louis, MO, USA). Briefly, cell death was induced by incubating 2×10^5 cells/ml with BAA-1 or BAA-2 for 60 min at concentrations corresponding to 1× IC_{50} after 8 h. Afterwards the cells were washed twice with phosphate buffered saline (PBS) and resuspended in the binding buffer. Fluorescein isothiocyanate (FITC) labeled annexin-V and PI was added, incubated for 10 min in the dark at room temperature and immediately analyzed with a FACSCalibur flow cytometer (Becton & Dickenson, San Jose, CA, USA) using the FL-1 and FL-3 channel. The apoptosis inducing substance tributyltin chloride (TBTC) was used at a concentration of 2 µM as positive control for apoptosis [16].

2.5. Caspase activity screening

To detect activation of caspases-1 to -10, an activity screen was performed using the Caspase Fluorometric Substrate Set II Plus kit (Biovision Research Products, Mountain View, CA, USA). Briefly, Ramos cells (2×10^5 cells/ml) were treated with 1× IC_{50} of BAA-1 or BAA-2 for 1 h, and for each caspase assayed, cells were lysed and supplemented with reaction buffer as well as DL-dithiothretiol solution. Subsequently, the 7-amino-4-trifluoro methylcoumarin conjugated caspase substrates were added, incubated at 37 °C for 2 h and analyzed on a fluorescence plate reader (SpectraMAX Gemini EM, Molecular devices, Sunnyvale, CA, USA). The increase in caspase activity was determined by comparing the fluorescence intensity with the levels of the non-treated control samples.

2.6. Transmission electron microscopy (TEM)

Ramos cells (2×10^5 cells/ml) were resuspended in serum free RPMI-1640 medium containing BAA-1 or BAA-2 and seeded in small culture flasks (NUNC Easy flask 25 cm^2, Thermo Fischer Scientific,

Langenselbold, Germany). The concentrations of BAA-1 and BAA-2 as well as incubation times were chosen according to the previously determined IC_{50} values. Treated cells and control cells were pre-fixed with Karnovsky's cacodylate-buffered (pH 7.2) formaldehyde–glutaraldehyde fixative at 4 °C overnight. The fixative was replaced by Karnovsky's buffer pH 7.4 and post-fixated with ferrocyanide-reduced osmium tetroxide. After dehydration in a graded series of ethanol, samples were infiltrated with a 1:1 mixture of acetonitrile and epon resin (AGAR 100, DDSA, MNA and DMP-30) overnight. Pure resin was applied the following day and then polymerized for 24 h. Ultrathin 70 nm sections were prepared and placed on formvar, carbon-stabilized copper grids. Uranyl acetate (5%) and Reynold's lead citrate were used for staining and contrasting. Samples were analyzed on a JEOL-1010 transmission electron microscope (JEOL, Akaishima, Japan) and images taken with an Olympus Morada side-mounted TEM CCD camera (Olympus soft imaging solutions GmbH, Münster, Germany).

2.7. Scanning electron microscopy (SEM)

The same incubation procedures were performed in the SEM studies as for the TEM preparations. For post-fixation, 1% osmium tetroxide in distilled water was used and dehydration was accomplished with a graded series of ethanol. Samples were subjected to chemical drying with hexamethyldisilazane. Specimens were mounted on aluminum stubs with carbon tape, and prior to examination sputter coated for 90 s. Samples were analyzed on a JEOL JSM-6300 scanning electron microscope (JEOL, Akaishima, Japan) and image acquisitions carried out via an EDAX Phoenix EDAM III data acquisition module (EDAX Inc., Mahwah, NJ, USA).

2.8. Mitochondrial membrane ($\Delta\Psi_m$) potential assessment

Ramos cells (2×10^5 cells/ml) were seeded in 12-well plates and incubated for 60 min with BAA-1 and BAA-2 at their determined IC_{50} values. Treatment with 2 μM TBTC was used as a positive control and untreated cells as a negative control. After 40 min tetramethylrhodamine ethyl ester perchlorate (TMRE) in DMSO was added to a final concentration of 100 nM and further incubated until the experiment end point. The cells were collected and resuspended in Hanks Balanced salt solution (HBSS) to a final concentration of 1×10^6 cells/ml and subsequently analyzed with a FACSCalibur flow cytometer.

2.9. Data analysis and software

Data sets were tested for statistically differences using the Wilcoxon Signed Rank test and Student's t-test (Sigma Plot software version 11; Systat Software Inc, San Jose, CA, USA). The same software was used to generate graphs. The FlowJo software version 7.6.1 (Tree Star Inc., Ashland, OR, USA) was used to create plots from the flow cytometry analysis. TEM images were acquired with help of the program iTEM version 5.0 (Olympus soft imaging solutions GmbH, Münster, Germany), and the program Genesis version 4.61 (EDAX Inc., Mahwah, NJ, USA) was used to acquire SEM images.

3. Results

3.1. Cell viability assay and IC_{50} determination

The IC_{50} values of BAA-1 and BAA-2 were determined by assaying the metabolic activity of Ramos cells using the redox indicator resazurin. During normal cellular respiration the dye is reduced from its blue species (resazurin) to an intense pink species (resorufin) and can therefore be used to assess metabolic activity and cytotoxicity [17]. A steady decrease of the IC_{50} values for both BAA-1 and BAA-2 was observed already after 1 h incubation leading to IC_{50} values of 8.1 ± 1.1 μg/ml for BAA-1 and 3.8 ± 0.7 μg/ml for BAA-2 after 8 h incubation (Fig. 2a). Continued incubation up to 24 h revealed no change in the IC_{50} values. Assaying doxorubicin in three independently performed experiments revealed an IC_{50} value of 1.7 ± 0.1 μg/ml against Ramos cells after a total time span of 28 h exposure to doxorubicin.

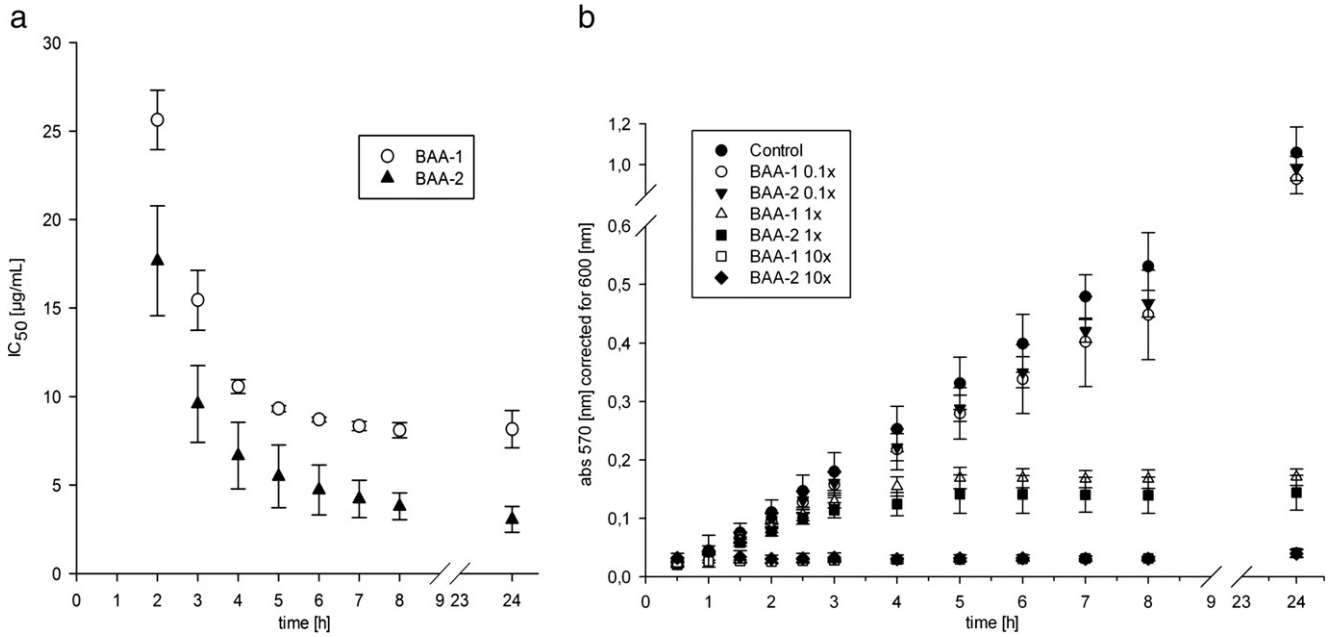

Fig. 2. a) Determination of IC_{50} values for BAA-1 and BAA-2 over a time range of 24 h by measuring the cell viability with the resazurin assay. No changes in IC_{50} values for BAA-1 or BAA-2 were observed after 8 h incubation and IC_{50} value of BAA-1 was determined to be 8.1 μg/ml and 3.8 μg/ml for BAA-2 (results display the mean ± SD of four independent experiments). b) Analysis of metabolic activity of Ramos cells treated with three different concentrations (0.1×, 1×, and 10× IC_{50}) of BAA-1 and BAA-2 for 24 h measured by absorbance of resorufin at 570 nm (results display the mean ± SD of three independent experiments).

3.2. Concentration dependent kinetic study

To investigate the impact of different concentrations of BAA-1 and BAA-2 on the viability and metabolic activity of Ramos cells over time, three different concentrations, i.e., 0.1×, 1×, and 10× of the determined IC_{50} values of BAA-1 and BAA-2 were chosen. A rapid inhibition of cell proliferation was detected already after 90 min for cells incubated with 10× the IC_{50} value of BAA-1 and BAA-2 (Fig. 2b). In contrast, cells incubated with 1× the IC_{50} value of BAA-1 and BAA-2 followed the profile of the control cells in the beginning of the experiment, but after 3 h the cellular viability decreased drastically and did not show any further changes throughout the experiment. Of note, for cells incubated with 0.1× the IC_{50} value was unaffected and followed the viability curve obtained for the control cells up to the 24 h endpoint of the experiment.

3.3. Detection of apoptosis and necrosis by flow cytometry

A hallmark of an early stage of apoptosis is the externalization of the phospholipid phosphatidylserine (PS) from the inner to the outer leaflet of the cell membrane [18]. During this stage the cell membrane integrity is still intact and the FITC labeled protein annexin-V is able to bind to PS on the cell surface and can be detected by flow cytometry. However, the positively charged PI is unable to enter and stain DNA in viable or early apoptotic cells, whereas late-stage apoptotic and necrotic cells are susceptible to both annexin-V-FITC and PI because of increased disintegration of the cell membrane [19]. Of note, Ramos cells treated with 1× IC_{50} of BAA-1 appeared unaffected, similarly as observed for the control cells and both the amount of annexin-V-FITC and PI positive cells was equally low as for the control cells (Fig. 3a and b). However, Ramos cells treated with 1× IC_{50} of BAA-2 showed an approximately 6.5-fold increased level of staining by annexin-V-FITC compared to the control cells, but no drastic increase in the PI signal (Fig. 3b). Cells treated with TBTC, which was used as positive control for apoptosis, showed a 9-fold increase in annexin-V-FITC positive cells. As shown in Fig. 3b, both the BAA-2 and TBTC treated cells differed from control cells regarding annexin-V-FITC labeling. In addition, membrane integrity was analyzed using PI as an indicator of membrane damage after incubation with 1× IC_{50} of BAA-1 and 1× IC_{50} of BAA-2 for 2 h. An almost 5-fold increase of PI uptake was observed for BAA-1 treated cells compared with controls and an almost 2.5-fold higher PI uptake

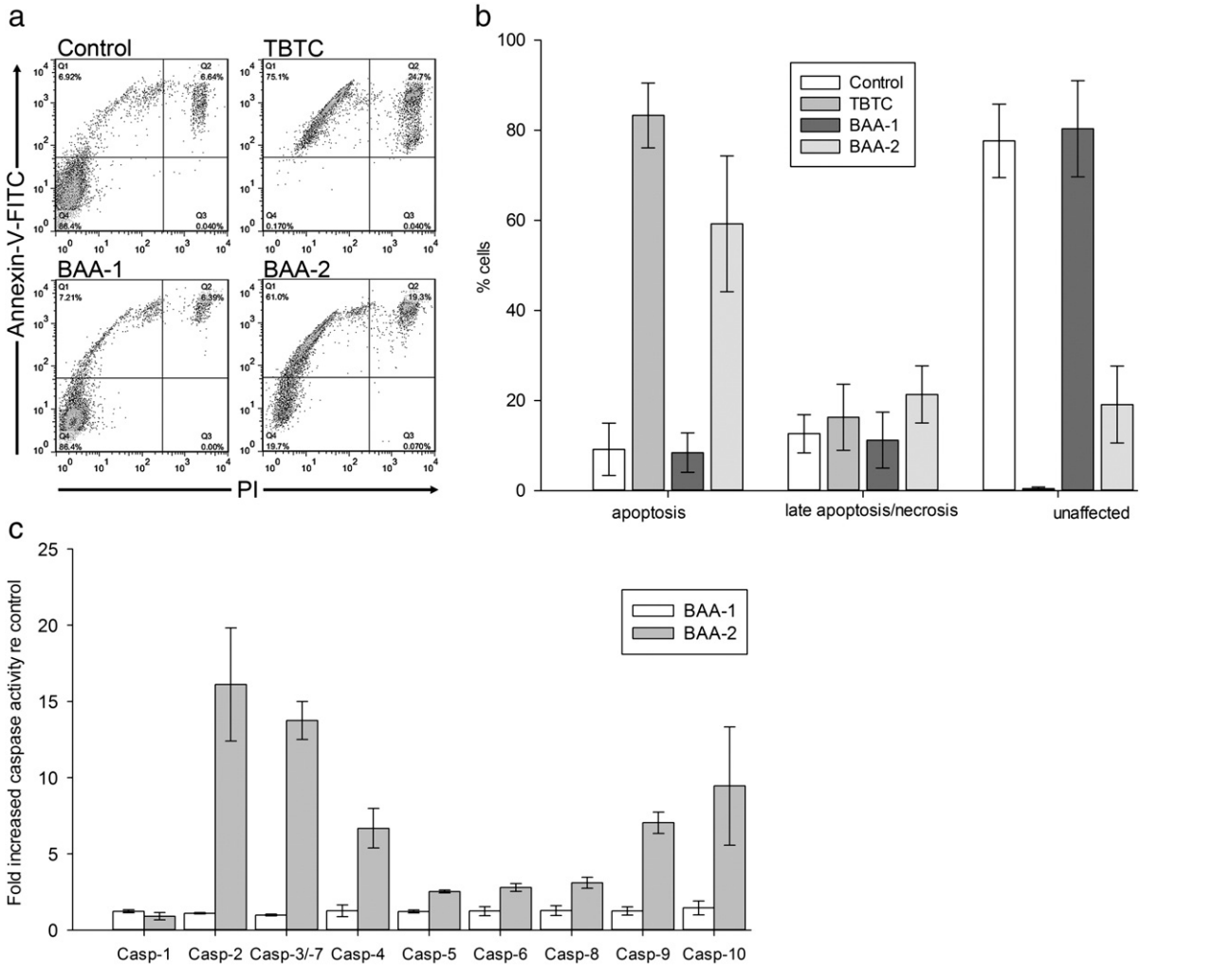

Fig. 3. a) Flow cytometry analysis of Ramos cells for detection of apoptosis (Q1), late-stage apoptosis and necrosis (Q2), or unaffected cells (Q4). Control cells and cells treated for 1 h with 1× IC_{50} concentration of BAA-1, BAA-2 or 2 μM TBTC. b) Quantification by flow cytometry of annexin-V-FITC and PI labeled Ramos cells for detection of apoptosis after 1 h incubation with BAA-1 and BAA-2 (results display the mean ± SD of three independent experiments). c) Activation of indicated caspases after 1 h incubation with 1× IC_{50} of BAA-1 (white bars) and BAA-2 (grey bars). The columns show increase in caspase activity relative to untreated control cells (results display the mean ± SD of three independent experiments).

when compared with BAA-2 treated cells (see supplementary data). Treatment of the cells with BAA-2 for 2 h did not result in any increase in PI uptake.

3.4. Caspase activity screening

Caspases are intracellular proteases that are activated during apoptosis [20]. The screening assessment of caspases-1 to -10 revealed that incubation of cell suspensions with 1× IC_{50} of BAA-2 for 1 h led to an activation of caspases-2 to -10, whereas no caspase activation was observed for cells incubated with 1× IC_{50} of BAA-1 (Fig. 3c). A shorter incubation period of 15 min did not show measurable caspase activation for BAA-2, and up to 2 h incubation did not lead to an increase in the caspase activation signal or shift in the signal pattern for BAA-1 or BAA-2 (data not shown). The strongest activation after treatment with BAA-2 was observed for activation of caspases-2, -3/-7, -4, -9 and -10 (Fig. 4). Western blotting for determination of cleaved caspase-3 was performed and verified the results from the fluorescence based caspase screening assay (data not shown).

3.5. Morphological analysis by electron microscopy

To further investigate the mechanism of action of BAA-1 and BAA-2, SEM and TEM studies were used to evaluate morphological changes in treated cells. Ramos cells were treated with 1× IC_{50} of BAA-1 and BAA-2 and subsequently fixed at 60, 120, 180, and 360 min. Untreated Ramos control cells were concurrently incubated for comparison and fixed at the experimental endpoint at 360 min (Fig. 4).

SEM images of the control cells (Fig. 4a and c) showed cells with a rough surface due to microvilli, which also were visible as fine membrane protrusions in the cross sections analyzed with TEM (Fig. 4b and d). The cell integrity of control cells was maintained during the experimental period of 360 min, and no sign of cell death was observed. The images of the control cells showed heterogenic nuclei with both eu- and heterochromatin.

By incubating Ramos cells with BAA-1 for 60 min the cells lost or retracted their microvilli, and membrane alterations were observed as craters or pore like structures (Fig. 4e). The TEM images demonstrated additional massive vacuolization in rounded cells without visible microvilli (Fig. 4f). However, no changes in chromatin appearance could be observed in cells treated with BAA-1. By prolonging the incubation time these effects became more drastic and cells clearly lost their membrane integrity and collapsed (Fig. 4i–j, m–n, and q–r).

When Ramos cells were incubated with BAA-2, the same morphological changes were observed with SEM as for BAA-1 (Fig. 4g–k), but in addition chromatin condensation was visible as a dark condensed ring along the nuclear envelope, thus indicating apoptotic processes (Fig. 4h, l, p and t) [21]. The cell integrity was maintained up to 180 min for Ramos cells treated with BAA-2 (Fig. 4o and p) but started disintegrating in the subsequent incubation period (Fig. 4s–t).

While organelles of the control cells and the 60 min BAA-1 treated cells displayed no differences, swollen or disrupted mitochondria were seen in the 60 min BAA-2 treated cells (Fig. 5u–w). Compared with healthy cells, mitochondria of the BAA-2 treated cells lost their inner structure of cristae and/or integrity of the outer mitochondrial membrane (Fig. 5u, w).

In addition 250 randomly selected control cells and cells treated for 60 min with BAA-1, as well as BAA-2, were counted and ranked in four categories, i.e. cells showing vacuolization with condensed chromatin, solely vacuolization, necrotic morphology and cells with no visible effects (Table 1).

Nearly 80% of the cells treated with BAA-1 could be categorized as cells containing vacuoles, whereas chromatin condensation was observed in less than 5% of the BAA-1 treated population. However, more than 60% of the cells treated with BAA-2 showed condensed

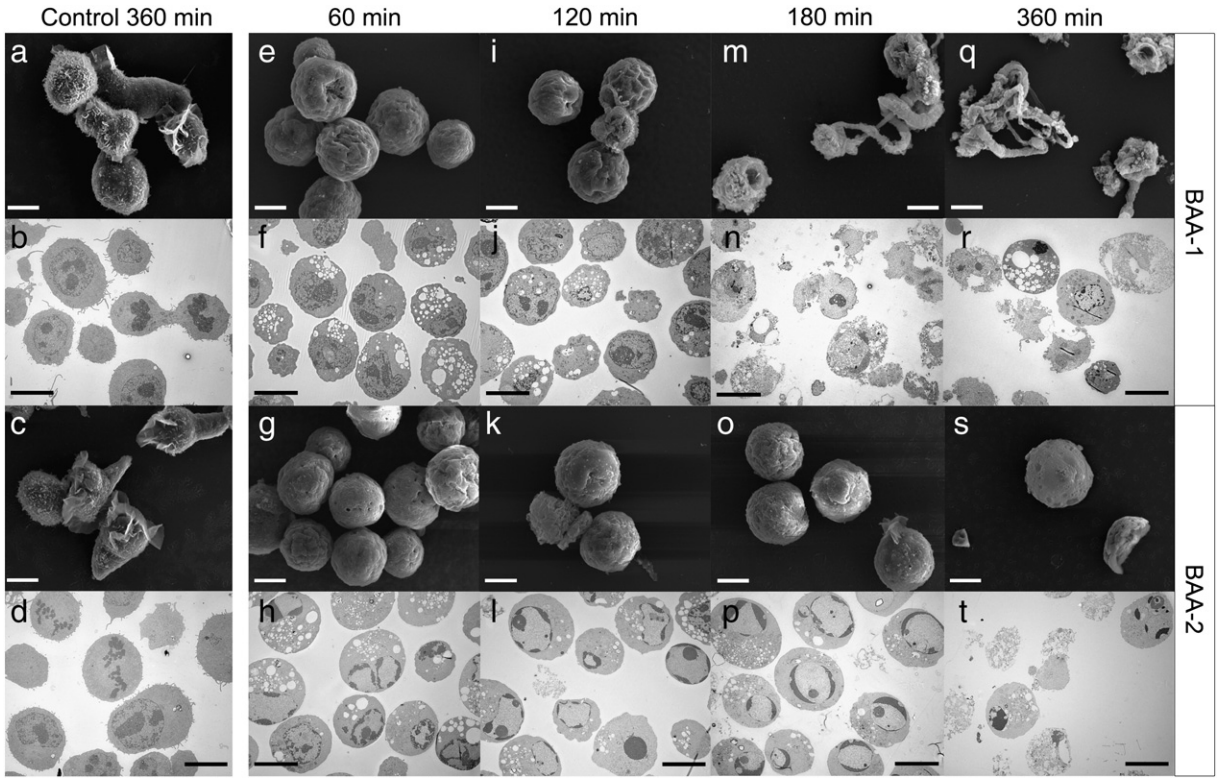

Fig. 4. SEM and TEM images of Ramos cells treated with BAA-1 and BAA-2, and compared with control cells incubated for 360 min (panels a–d). Cells treated with 1× IC_{50} of BAA-1 for 60 min (e–f), 120 min (i–j), 180 min (m–n) and 360 min (q–r). Cells treated with 1× IC_{50} of BAA-2 treated for 60 min (g–h), 120 min (k–l), 180 min (o–p) and 360 min (s–t). Scale bar SEM 5 μm, and scale bar TEM 10 μm (a–t).

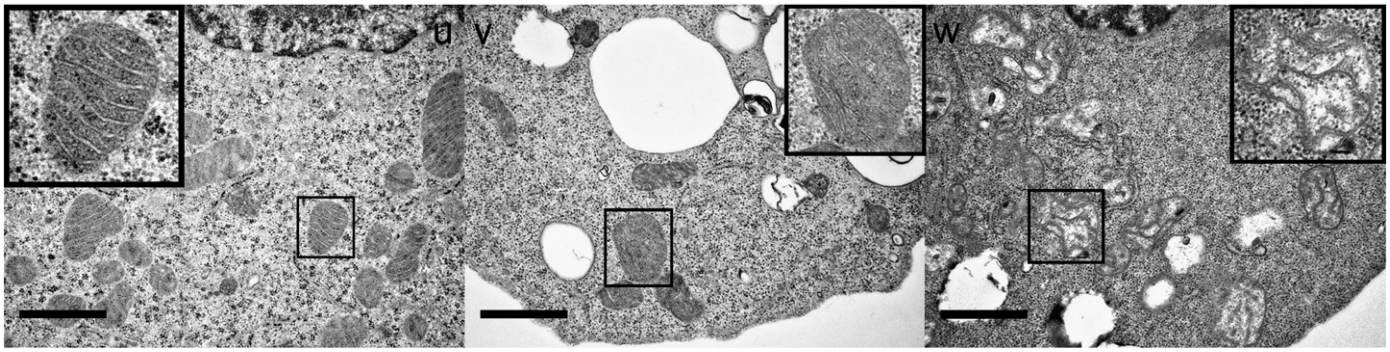

Fig. 5. Morphology of mitochondria in untreated control cells (u), for 60 min with BAA-1 treated cells (v) and for 60 min BAA-2 treated cells (w). Scale bar 1 μm.

chromatin together with strong vacuolization, while 20% demonstrated just vacuolization. Among the control cells more than 90% were unaffected, and less than 10% showed alterations such as apoptotic or necrotic morphology.

3.6. Mitochondrial membrane potential assessment ($\Delta\Psi_m$)

Loss of mitochondrial membrane potential has been reported to be connected to mitochondrial outer membrane permeabilization, a process occurring during activation of the intrinsic pathway of apoptosis [22]. Based on the TEM findings and to further investigate the mechanism of action of BAA-1 and BAA-2, the integrity of the mitochondrial membrane potential ($\Delta\Psi_m$) was assessed using TMRE staining and flow cytometry (Fig. 6). As already suggested from analyses of the TEM images, no differences between the control cells and the BAA-1 treated cells were observed. However, by incubating cells with BAA-2 less than 25% of the cells showed an intact $\Delta\Psi_m$. TBTC was used as positive control due to its ability to induce a complete collapse of the $\Delta\Psi_m$ in all cells resulting in two peaks.

4. Discussion

Insights into the interaction of ACPs with mammalian cells are still very limited, and it is not just beneficial but also crucial to focus on detailed studies on mechanisms of action to succeed in developing novel anticancer agents in the field of AMP research [23]. We have in the present study investigated the anticancer mechanism of action of two newly developed $\beta^{2,2}$-amino acid derivatives, BAA-1 and BAA-2, that were originally designed to confirm the pharmacophore model of short cationic AMPs against multi-resistant *S. aureus* (14).

At first the cytotoxic properties of BAA-1 and BAA-2 were determined against the human Burkitt's lymphoma cell line Ramos using a resazurin-based toxicity assay. The resazurin assay also made it possible to determine the IC_{50} values by simultaneous incubation of resazurin and the two $\beta^{2,2}$-amino acid derivatives, which showed that BAA-2 (IC_{50} 3.8 μg/ml) was twice as potent as BAA-1 (IC_{50} 8.1 μg/ml) (Fig. 2a). The results revealed furthermore that the $\beta^{2,2}$-amino acid derivatives BAA-1 and BAA-2 had an immediate impact on Ramos cancer cells, whereas the antitumor drug doxorubicin required a much longer incubation time due to its intercalating

Table 1
Categorization of randomly selected cells based on cell morphology events observed using TEM (in %). Untreated control cells and cells treated with BAA-1 or BAA-2 for 60 min were evaluated.

	unaff	vac	nec	chr
Control	91.6	2.4	3.6	2.4
BAA-1	18.4	75.6	1.6	4.4
BAA-2	6.8	21.2	7.6	64.4

Abbreviations: unaffected (unaff); vacuolization (vac); necrosis (nec); condensed chromatin (chr).

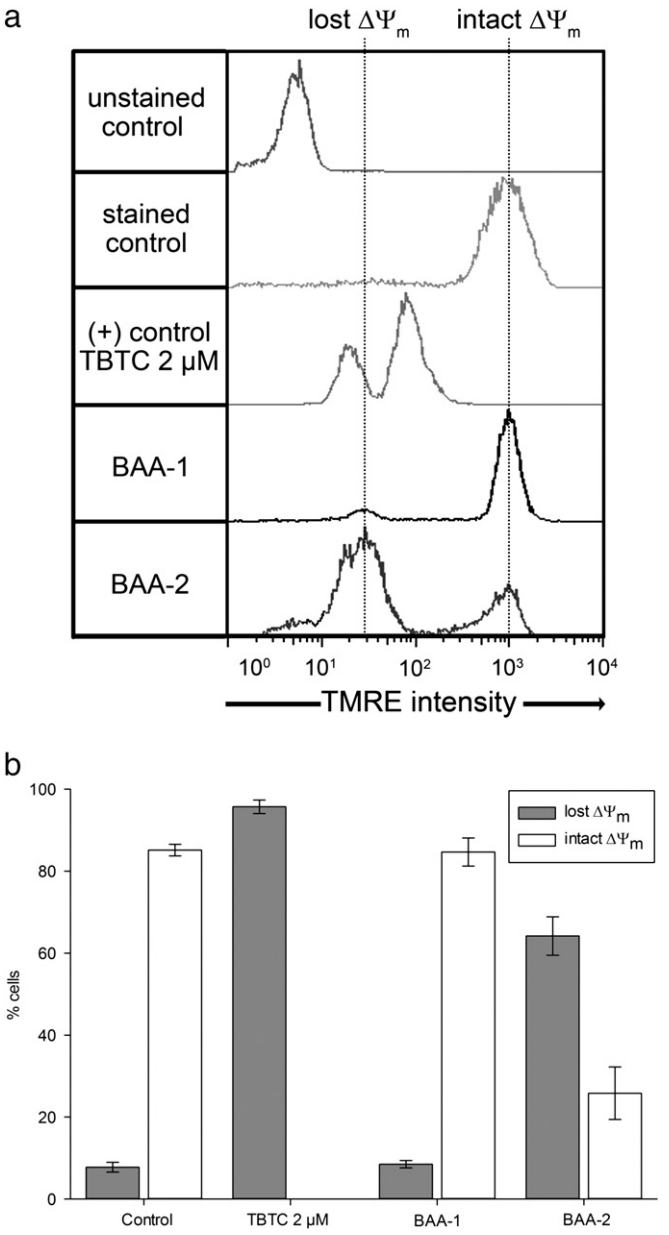

Fig. 6. Representative histograms of the mitochondrial membrane potential assessment and quantification by flow cytometry. a) TMRE stained control cells as well as cells treated with BAA-1 displayed intact $\Delta\Psi_m$ while unstained control cells, cells treated with 2 μM TBTC or BAA-2 showed no or lower TMRE intensity, i.e. decreased or absent $\Delta\Psi_m$ upon treatment, as indicated by a peak shift to the left. b) Three independently performed experiments showed a remarkable difference between untreated and BAA-2 treated cells, while BAA-1 had no impact on $\Delta\Psi_m$ (results display the mean ± SD).

mechanism of action. In fact we were unable to use the same cytotoxicity assay for doxorubicin as for BAA-1 and BAA-2. Even with the highest doxorubicin concentration we could not determine an IC_{50} value after 8 h incubation and therefore had to modify the assay setup. As described in the Material and methods section, a 24 h pretreatment with doxorubicin and subsequent assaying with resazurin led to an IC_{50} value of 1.7 μg/ml. Both BAA-1 and BAA-2 thereby displayed anticancer potencies comparable with the wide spectrum antitumor drug doxorubicin [24], and were equally or even more potent than recently reported for much larger anticancer AMPs consisting of 18 or 37 amino acids [10–13,24].

In addition, the resazurin assay allowed us to follow the impact of different concentrations of the $\beta^{2,2}$-amino acid derivatives on Ramos cells over a 24 h time period, which provided valuable information on potency and rapidness of the substances (Fig. 2b). The first 3 h of incubation and with concentrations equal to the IC_{50} value determined after 8 h already had a severe impact on cell survival. We therefore believe that this constellation of both time frame and compound concentrations were appropriate for further experiments, and subsequent studies were therefore set up according to our kinetic assay. In addition, no differences in the curve profile between BAA-1 and BAA-2 were observed when used at their half inhibitory concentrations suggesting similar cell killing properties (Fig. 2b). Of note, low concentrations ($0.1\times$ IC_{50}) of BAA-1 and BAA-2 seemed not to affect cell survival at all, while the very high concentrations ($10\times$ IC_{50}) of BAA-1 and BAA-2 caused rapid cell death. Hence, both the lowest and highest test concentrations were disregarded with respect to further experiments.

To determine differences in cell death induced by BAA-1 and BAA-2, treated cells were stained with annexin-V-FITC/PI and analyzed by flow cytometry. The results showed that BAA-1 treated cells hardly differed from the untreated control cells after 1 h incubation, whereas BAA-2 treated cells displayed a similar staining pattern as cells incubated with our positive control TBTC, indicating an induction of apoptosis (Fig. 3a–b). It is worth noting that the membrane integrity was not extensively affected after 1 h of incubation with either BAA-1 or BAA-2, even though the cancer cell membrane is the target of many AMP based anticancer peptides [25]. Both annexin-V-FITC labeling of PS on the cytosolic side of the cells and PI signals were comparatively low with respect to the control cells and indicated no severe membrane damage. Similar observations were reported by Cerón et al. who incubated HL-60 leukemia cells with the AMP cecropin A at its IC_{50} and performed annexin-V-FITC/PI labeling as well as measuring the release of lactate dehydrogenase [10]. An increased PI uptake was however observed for BAA-1 treated cells when the incubation time was prolonged to 2 h (see supplementary data).

Although we have recently reported membranolytic effects on *S. aureus* when incubated with BAA-2, the membrane component cholesterol has been suspected to alter membrane stability, thus making non-malignant, eukaryotic cells less prone to peptide membrane interaction compared to bacterial cell membranes where cholesterol is basically absent [9,26]. The reason that cationic ACPs nevertheless preferably interact with cancer cells is most likely due to an overexpression of negative membrane constituents and an increased amount of microvilli resulting in a larger surface area compared to non-malignant cells [25].

A caspase assay was performed to further elucidate the mechanisms of cell death and to get more insights regarding possible intracellular targets. The analyses were not just focused on the commonly performed screens for caspases involved in the two major apoptosis pathways (caspases-3, -8 and -9), but included also downstream caspases as well as inflammation-associated caspases. Only BAA-2 leads to caspase activation in the treated cells and even doubling of the incubation time for BAA-1 had no impact on the caspase activation levels, thus supporting the annexin-V-FITC/PI flow cytometer results regarding the hypothesis of two different mechanisms of action for BAA-1 and BAA-2 (Fig. 3c). Treatment with BAA-2 resulted in activation of caspases-2, -3/-7, -6, -9, -10, suggesting an induction of the intrinsic apoptotic pathway [27]. Similar results have been reported for the much longer AMP bovine lactoferricin (Lfcin B), in which Eliassen et. al reported activation of caspases-6, -7, and -9 as well as up-regulation of caspase-3 upon incubation with Lfcin B in neuroblastoma cells [28]. Mader et al. observed cleavage of procaspases-2, -3 and -9 by treating Jurkat T leukemia cells with Lfcin B, however no caspase activation was found when apoptosis was induced in Ramos or Raji B-lymphoma cells [29,30]. Also the peptides epinecidine-1, buforin IIb and a series of mitochondria targeting peptides activate caspases by the intrinsic pathway [31–33]. However, treatment with BAA-2 also resulted in an elevated level of activated caspase-4, which is located in the membrane of the endoplasmatic reticulum (ER) and is reported in context of ER stress [34]. Of note, Rosati and co-workers reported that ER stress can lead to mitochondrial cytochrome C release, apoptosome formation and initiation of the caspase cascade of the intrinsic pathway in B-chronic lymphocytic leukemia (BCLL) cells [35].

To investigate which apoptotic pathway BAA-2 induced and to what extent caspase-4 was involved, experiments using inhibitors for caspases-3, -4, -8, and -9 were also addressed in the study. Several attempts were undertaken to titrate inhibitor concentrations, but contrary to our expectations of increased cell survival, the pretreatment with caspase inhibitors decreased overall cell survival or had no effect at all (data not shown). The inhibitors therefore seemed to make the Ramos cells more susceptible to BAA-2 treatment and had a negative impact on cell survival, which is also reported by others [36,37]. The impact of activated caspase-4 could therefore not be revealed. However, direct interactions with negatively charged lipids in the ER membrane and subsequent release and activation of the ER bound caspase-4 is possible [38].

Electron microscopy and assessment of the mitochondrial potential are important tools to further study the apoptotic pathway, the impact on mitochondria, and the results of caspase activation upon AMP cancer cell treatment. Since apoptosis and necrosis are accompanied by distinct changes in morphology, both intracellularly and on the cell surface, SEM and TEM were applied to verify the bioassay based results [39]. As an early effect, treating Ramos cells with BAA-1 or BAA-2 resulted in loss of microvilli and a rounding up of the Ramos cells (Fig. 4). These characteristic changes have been reported and reviewed in context of apoptosis by others [40,41]. After 3 h of incubation with BAA-1, the cells lost their integrity and necrotic cell bodies were observed. In contrast to BAA-1, Ramos cells treated with BAA-2 maintained their integrity up to 3 h and necrosis was finally observed 6 h past onset of incubation.

By using TEM for analysis of effects on intracellular structures, we observed the same degree of vacuolization in both BAA-1 and BAA-2 treated cells. These pronounced intracellular changes compared to the control cells were not associated with a loss of cell membrane integrity since PI staining in the flow cytometry experiments showed intact cell membranes after 1 h incubation with BAA-1 and BAA-2. Hence, these findings may indicate both cell penetrating properties and direct membrane interactions for BAA-1 and BAA-2.

Increased vacuolization has been reported to occur in cells degrading toxic cytoplasmic constituents via autophagic processes [42]. These processes involving vacuolization should, however, rather be seen in context of running a survival program than a mechanism or initiation of cell death [42,43]. However, the lack of cell material inside the vacuoles and difficulties in finding defined double layers surrounding these vacuoles could indicate a TEM preparation artifact. As described by Eskelinen, cell membrane invaginations, as we observed in the SEM images, can lead to vacuole appearance due to the preparation of ultra-sections prior to examination by TEM [44]. Beside the

similarities regarding vacuolization, characteristic half-moon shaped chromatin condensation patterns, increasing over time and typical for apoptosis, were observed for BAA-2 treated cells [21]. Our TEM images supported the data acquired by flow cytometry, since chromatin condensation has been reported to occur concurrently with phosphatidylserine externalization in B-cells, thus leading to annexin-V-FITC staining [45]. Similar morphological changes were reported for the 27 amino acid AMP pep27anal2 where Jurkat cells were treated with almost 3× the IC_{50} value over a time range of 4 h [46]. Lee et al. also observed 30% increase in apoptosis after cell treatment with pep27anal2, whereas in our case incubation with 1× IC_{50} of BAA-2 resulted in 60% apoptotic cells already after 1 h. The percentage of BAA-2 treated cells in apoptotic stage was additionally confirmed by counting 250 randomly chosen cells and categorizing differences in cell morphology. The results showed that 1 h treatment with BAA-2 resulted in more than 60% apoptotic cells with condensed chromatin, whereas similar treatment with BAA-1 did not alter chromatin appearance compared to the control cells (Table 1).

TEM images with higher magnification were also studied to evaluate the involvement of mitochondria in the cell death scenarios upon treatment with BAA-1 and BAA-2. The micrographs revealed no ultra-structural differences of the mitochondria in the control cells or BAA-1 treated cells, while pronounced mitochondrial changes were observed in cells treated with BAA-2 (Fig. 5, panels u–w). Disintegration processes of the outer mitochondrial membrane as well as the cristae were visible, and suggested a direct mechanism of BAA-2 on mitochondria.

To verify these TEM findings the mitochondrial membrane potential was assessed using TMRE. The dye accumulated in mitochondria of the control cells and BAA-1 treated cells, while cells incubated with BAA-2 displayed an almost 60% decrease in TMRE staining compared to the control cells, indicating mitochondrial outer membrane permeabilization (Fig. 6). A complete disappearance of staining was seen for our positive control TBTC, which is reported to interact with mitochondria via two mechanisms causing an immediate but slow loss of $\Delta\Psi_m$, and a mechanism involving mitochondrial permeability transition pore formation, with a rapid loss of $\Delta\Psi_m$ and release of cytochrome C [47]. As described above, similar results were reported for Lfcin B and other types of ACPs causing swelling of the mitochondria and release of apoptogenic factors [28,29,31,48]. We therefore suggest the mechanism of BAA-2 to involve a direct interaction with the mitochondria causing release of apoptosis promoting factors such as cytochrome C and subsequent activation of caspase-9 and downstream caspases leading to apoptotic cell death [20,22]. BAA-2 might also have increased ability to penetrate the cell membrane by passive diffusion and being subsequently attracted to the mitochondria due to their net negative surface charge. We have previously reported that BAA-2 derivatives are able to permeate through a phospholipid vesicle based barrier without destroying the phospholipid bilayers, hence strengthening this hypothesis [9]. Interestingly, the caspase inhibitors were not able to abolish the BAA-2 induced cell death which could suggest a caspase-independent cell death mechanism. The observed extensive damage of the mitochondria could lead to fast ATP depletion and liberation of the presumably uncleaved apoptosis-inducing factor (AIF) from the inner mitochondrial membrane [49]. Lethal PARP-1 activation may follow the AIF release and could lead to a cell death mechanism called parthanatos. This type of cell death is from a morphological and biochemical point of view very similar to apoptosis however it does not involve caspase activation [50]. This caspase independent, but controlled, cell death mechanism would be an interesting aspect concerning therapy improvement of apoptosis resistant cancers [51].

Since neither the biochemical assays nor the electron microscopy studies gave positive results for apoptosis by BAA-1 treatment, we infer that the mechanism of BAA-1 involves time dependent membrane-lytic processes leading to necrotic cell death. Based on our flow cytometry studies and morphological observations we further suggest that BAA-1 was to a lower extent able to permeate the cell membrane, but rather promotes membrane lysis. It is therefore reasonable to believe that when a certain trigger concentration is reached, the cancer cell membrane is not able to tolerate more BAA-1 insertions and collapses. However, one has to take into consideration that both, potency and the mechanism of action, may vary when using different cell lines as reported for the AMP Lfcin B. Fadnes et al. have demonstrated that the cell killing properties of Lfcin B differed when cells of different origin were assessed [52]. Furthermore, as described above, the Rekdal and Hoskin groups have reported different cancer cell killing mechanisms of LfcinB [28–30]. Since fluorescence labeling of the compounds would alter their properties too drastically due to their small size, time dependent permeability experiments on model membranes could reveal penetration properties of the two compounds as well as their abilities to destabilize a phospholipid bilayer. We are currently commencing more mechanistic studies to gain a better understanding of the compounds and their interactions with various membranes.

5. Conclusions

Taken together, we suggest dissimilar modes of action of the two structurally related $\beta^{2,2}$-amino acid derivatives, in which BAA-1 induced cell death of Ramos cells by necrosis, whereas BAA-2 induced apoptotic cell death via a mitochondria mediated activation of caspases of the intrinsic pathway. Even though the structural differences of BAA-1 and BAA-2 appear to be rather marginal, they have however a considerable impact on cell killing properties. Further exploration of the structure and mechanism of action relationship of $\beta^{2,2}$-amino acid derivatives might aid in the design of specific small ACPs in future.

Conflict of interest statement

No conflict of interest is declared.

Acknowledgements

We like to thank Prof. Øystein Rekdal for kindly providing the Ramos cell line and the Bioimaging Platform, University of Tromsø for providing access to laboratories and instruments. In addition we would like to thank the Electron Microscopy Department, University of Tromsø for preparation of the ultra-thin sections and access to laboratories and microscopes. The authors would also like to express their thanks to Dr. Peter McCourt for linguistic revision of the manuscript.

Appendix A. Supplementary data

Supplementary data to this article can be found online at http://dx.doi.org/10.1016/j.bbamem.2012.07.005.

References

[1] J. Stephenson, Cancer no. 1 killer by 2010, J. Am. Med. Assoc. 301 (2009) 263.
[2] P. Boyle, B. Levin, World Cancer Report, IARC Press, Lyon, 2008.
[3] A. Giuliani, G. Pirri, S.F. Nicoletto, Antimicrobial peptides: an overview of a promising class of therapeutics, Cent. Eur. J. Biol. 2 (2007) 1–33.
[4] D.W. Hoskin, A. Ramamoorthy, Studies on anticancer activities of antimicrobial peptides, Biochim. Biophys. Acta Biomembr. 1778 (2008) 357–375.
[5] G.M. Cragg, P.G. Grothaus, D.J. Newman, Impact of natural products on developing new anti-cancer agents, Chem. Rev. 109 (2009) 3012–3043 (Washington, DC, US).
[6] S. Al-Benna, Y. Shai, F. Jacobsen, L. Steinstraesser, Oncolytic activities of host defense peptides, Int. J. Mol. Sci. 12 (2011) 8027–8051.

[7] F. Schweizer, Cationic amphiphilic peptides with cancer-selective toxicity, Eur. J. Pharmacol. 625 (2009) 190–194.
[8] T. Hansen, T. Alst, M. Havelkova, M.B. Strøm, Antimicrobial activity of small beta-peptidomimetics based on the pharmacophore model of short cationic antimicrobial peptides, J. Med. Chem. 53 (2010) 595–606.
[9] T. Hansen, D. Ausbacher, G.E. Flaten, M. Havelkova, M.B. Strøm, Synthesis of cationic antimicrobial beta 2,2-amino acid derivatives with potential for oral administration, J. Med. Chem. 54 (2011) 858–868.
[10] J.M. Ceron, J. Contreras-Moreno, E. Puertollano, G. Alvarez de Cienfuegos, M.A. Puertollano, M.A. de Pablo, The antimicrobial peptide cecropin A induces caspase-independent cell death in human promyelocytic leukemia cells, Peptides 31 (2010) 1494–1503.
[11] Y.Q. Chen, C. Min, M. Sang, Y.Y. Han, X. Ma, X.Q. Xue, S.Q. Zhang, A cationic amphiphilic peptide ABP-CM4 exhibits selective cytotoxicity against leukemia cells, Peptides 31 (2010) 1504–1510.
[12] Y.b. Huang, X.f. Wang, H.y. Wang, Y. Liu, Y. Chen, Studies on mechanism of action of anticancer peptides by modulation of hydrophobicity within a defined structural framework, Mol. Cancer Ther. 10 (2011) 416–426.
[13] C. Tang, X. Shao, B. Sun, W. Huang, F. Qiu, Y. Chen, Y.K. Shi, E.Y. Zhang, C. Wang, X. Zhao, Anticancer mechanism of peptide P18 in human leukemia K562 cells, Org. Biomol. Chem. 8 (2010) 984–987.
[14] C.A. Lipinski, F. Lombardo, B.W. Dominy, P.J. Feeney, Experimental and computational approaches to estimate solubility and permeability in drug discovery and development settings, Adv. Drug Deliv. Rev. 23 (1997) 3–25.
[15] D.A. Gewirtz, A critical evaluation of the mechanisms of action proposed for the antitumor effects of the anthracycline antibiotics adriamycin and daunorubicin, Biochem. Pharmacol. 57 (1999) 727–741.
[16] H. Stridh, I. Cotgreave, M. Mueller, S. Orrenius, D. Gigliotti, Organotin-induced caspase activation and apoptosis in human peripheral blood lymphocytes, Chem. Res. Toxicol. 14 (2001) 791–798.
[17] J. O'Brien, I. Wilson, T. Orton, F. Pognan, Investigation of the Alamar Blue (resazurin) fluorescent dye for the assessment of mammalian cell cytotoxicity, Eur. J. Biochem. 267 (2000) 5421–5426.
[18] S. Martin, C.P.M. Reutelingsperger, A.J. McGahon, J.A. Rader, R.C.A.A. van Schie, D.M. LaFace, D.R. Green, Early redistribution of plasma membrane phosphatidylserine is a general feature of apoptosis regardless of the initiating stimulus: inhibition by overexpression of Bcl-2 and Abl, J. Exp. Med. 182 (1995) 1545–1556.
[19] M.G. Ormerod, X.M. Sun, D. Brown, R.T. Snowden, G.M. Cohen, Quantification of apoptosis and necrosis by flow cytometry, Acta Oncol. 32 (1993) 417–424.
[20] M. Kurokawa, S. Kornbluth, Caspases and kinases in a death grip, Cell 138 (2009) 838–854.
[21] J.F. Kerr, A.H. Wyllie, A.R. Currie, Apoptosis: a basic biological phenomenon with wide-ranging implications in tissue kinetics, Br. J. Cancer 26 (1972) 239–257.
[22] D.R. Green, G. Kroemer, The pathophysiology of mitochondrial cell death, Science 305 (2004) 626–629.
[23] K. Matsuzaki, Control of cell selectivity of antimicrobial peptides, Biochim. Biophys. Acta Biomembr. 1788 (2009) 1687–1692.
[24] R.B. Weiss, The anthracyclines: will we even find a better doxorubicin? Semin. Oncol. 19 (1992) 670–686.
[25] S. Riedl, D. Zweytick, K. Lohner, Membrane-active host defense peptides—challenges and perspectives for the development of novel anticancer drugs, Chem. Phys. Lipids 164 (2011) 766–781.
[26] O.G. Mouritsen, M.J. Zuckermann, What's so special about cholesterol? Lipids 39 (2004) 1101–1113.
[27] E.A. Slee, C. Adrain, S.J. Martin, Serial killers: ordering caspase activation events in apoptosis, Cell Death Differ. 6 (1999) 1067–1074.
[28] L.T. Eliassen, G. Berge, A. Leknessund, M. Wikman, I. Lindin, C. Loekke, F. Ponthan, J.I. Johnsen, B. Sveinbjoernsson, P. Kogner, T. Flaegstad, Ø. Rekdal, The antimicrobial peptide, lactoferricin B, is cytotoxic to neuroblastoma cells in vitro and inhibits xenograft growth in vivo, Int. J. Cancer 119 (2006) 493–500.
[29] J.S. Mader, J. Salsman, D.M. Conrad, D.W. Hoskin, Bovine lactoferricin selectively induces apoptosis in human leukemia and carcinoma cell lines, Mol. Cancer Ther. 4 (2005) 612–624.
[30] S.J. Furlong, J.S. Mader, D.W. Hoskin, Bovine lactoferricin induces caspase-independent apoptosis in human B-lymphoma cells and extends the survival of immune-deficient mice bearing B-lymphoma xenografts, Exp. Mol. Pathol. 88 (2010) 371–375.
[31] K.L. Horton, S.O. Kelley, Engineered apoptosis-inducing peptides with enhanced mitochondrial localization and potency, J. Med. Chem. 52 (2009) 3293–3299.
[32] J.Y. Chen, W.J. Lin, J.L. Wu, G.M. Her, C.F. Hui, Epinecidin-1 peptide induces apoptosis which enhances antitumor effects in human leukemia U937 cells, Peptides 30 (2009) 2365–2373.
[33] H.S. Lee, C.B. Park, J.M. Kim, S.A. Jang, I.Y. Park, M.S. Kim, J.H. Cho, S.C. Kim, Mechanism of anticancer activity of buforin IIb, a histone H2A-derived peptide, Cancer Lett. 271 (2008) 47–55.
[34] J. Hitomi, T. Katayama, Y. Eguchi, T. Kudo, M. Taniguchi, Y. Koyama, T. Manabe, S. Yamagishi, Y. Bando, K. Imaizumi, Y. Tsujimoto, M. Tohyama, Involvement of caspase-4 in endoplasmic reticulum stress-induced apoptosis and Abeta-induced cell death, J. Cell Biol. 165 (2004) 347–356.
[35] E. Rosati, R. Sabatini, G. Rampino, F. De Falco, M. Di Ianni, F. Falzetti, K. Fettucciari, A. Bartoli, I. Screpanti, P. Marconi, Novel targets for endoplasmic reticulum stress-induced apoptosis in B-CLL, Blood 116 (2010) 2713–2723.
[36] N. Shah, R.J. Asch, A.S. Lysholm, T.W. LeBien, Enhancement of stress-induced apoptosis in B-lineage cells by caspase-9 inhibitor, Blood 104 (2004) 2873–2878.
[37] D. Vercammen, R. Beyaert, G. Denecker, V. Goossens, G. Van Loo, W. Declercq, J. Grooten, W. Fiers, P. Vandenabeele, Inhibition of caspases increases the sensitivity of L929 cells to necrosis mediated by tumor necrosis factor, J. Exp. Med. 187 (1998) 1477–1485.
[38] G. van Meer, D.R. Voelker, G.W. Feigenson, Membrane lipids: where they are and how they behave, Nat. Rev. Mol. Cell Biol. 9 (2008) 112–124.
[39] J.F. Kerr, G.C. Gobe, C.M. Winterford, B.V. Harmon, Anatomical methods in cell death, Methods Cell Biol. 46 (1995) 1–27.
[40] G. Hacker, The morphology of apoptosis, Cell Tissue Res. 301 (2000) 5–17.
[41] D.V. Krysko, T. Vanden Berghe, K. D'Herde, P. Vandenabeele, Apoptosis and necrosis: detection, discrimination and phagocytosis, Methods 44 (2008) 205–221.
[42] G. Kroemer, B. Levine, Autophagic cell death: the story of a misnomer, Nat. Rev. Mol. Cell Biol. 9 (2008) 1004–1010.
[43] B. Levine, J. Yuan, Autophagy in cell death: an innocent convict? J. Clin. Invest. 116 (2006) 2679–2688.
[44] E. Eskelinen, To be or not to be? Examples of incorrect identification of autophagic compartments in conventional transmission electron microscopy of mammalian cells, Autophagy 4 (2008) 257–260.
[45] G. Koopman, C.P.M. Reutelingsperger, G.A.M. Kuijten, R.M.J. Keehnen, S.T. Pals, M.H.J. van Oers, Annexin V for flow cytometric detection of phosphatidylserine expression on B cells undergoing apoptosis, Blood 84 (1994) 1415–1420.
[46] D.G. Lee, K.S. Hahm, Y. Park, H.Y. Kim, W. Lee, S.C. Lim, Y.K. Seo, C.H. Choi, Functional and structural characteristics of anticancer peptide Pep27 analogues, Cancer Cell Int. 5 (2005) 21.
[47] V. Gogvadze, H. Stridh, S. Orrenius, I. Cotgreave, Tributyltin causes cytochrome c release from isolated mitochondria by two discrete mechanisms, Biochem. Biophys. Res. Commun. 292 (2002) 904–908.
[48] R. Smolarczyk, T. Cichon, W. Kamysz, M. Glowala-Kosinska, A. Szydlo, L. Szultka, A.L. Sieron, S. Szala, Anticancer effects of CAMEL peptide, Lab Invest. 90 (2010) 940–952.
[49] L. Delavallee, L. Cabon, P. Galan-Malo, H.K. Lorenzo, S.A. Susin, AIF-mediated caspase-independent necroptosis: a new chance for targeted therapeutics, IUBMB Life 63 (2011) 221–232.
[50] Y. Wang, V.L. Dawson, T.M. Dawson, Poly(ADP-ribose) signals to mitochondrial AIF: a key event in parthanatos, Exp. Neurol. 218 (2009) 193–202.
[51] P. Kreuzaler, C.J. Watson, Killing a cancer: what are the alternatives? Nat. Rev. Cancer 12 (2012) 411–424.
[52] B. Fadnes, Ø. Rekdal, L. Uhlin-Hansen, The anticancer activity of lytic peptides is inhibited by heparan sulfate on the surface of the tumor cells, BMC Cancer 9 (2009) 183.